Supporting information

to

Easy access to Fe_2N nanomaterials from Fe nanocrystals and investigation of their electrocatalytic properties for the water electrolysis and CO_2 reduction

Azadeh EDALAT,[1,2] Laure VENDIER,[1] Catherine AMIENS,[1]* Marc RESPAUD,[2] Pierre ROBLIN,[3] Jérôme ESVAN,[4] Quyen T. NGUYEN,[5] Duc N. NGUYEN,[5] Vu T. TRAN,[5] Ly T. Le,[5] Phong D. TRAN,[5]* Frederic DUMESTRE[6]

[1] Université de Toulouse, CNRS, LCC, 205 Route de Narbonne, BP 44099, F-31077 Toulouse Cedex 4, France
[2] Université de Toulouse, CNRS, CEMES, 29 rue Jeanne Marvig, F-31055 Toulouse, France
[3] Laboratoire de Génie Chimique, Université de Toulouse, CNRS, INPT, UPS, 118, route de Narbonne, Toulouse, 31062, France
[4] Centre Inter-universitaire de Recherche et d'Ingénierie des Matériaux, INP-ENSIACET, CNRS, Université de Toulouse, 118, route de Narbonne, 31062 Toulouse, France
[5] University of Science and Technology of Hanoi, Vietnam Academy of Science and Technology, 18 Hoang Quoc Viet, Cau Giay, Hanoi, Viet Nam
[6] Nanomeps, Département Génie Physique INSA, 135 avenue de Rangueil, 31 077 TOULOUSE Cedex 4, FRANCE

Table of contents

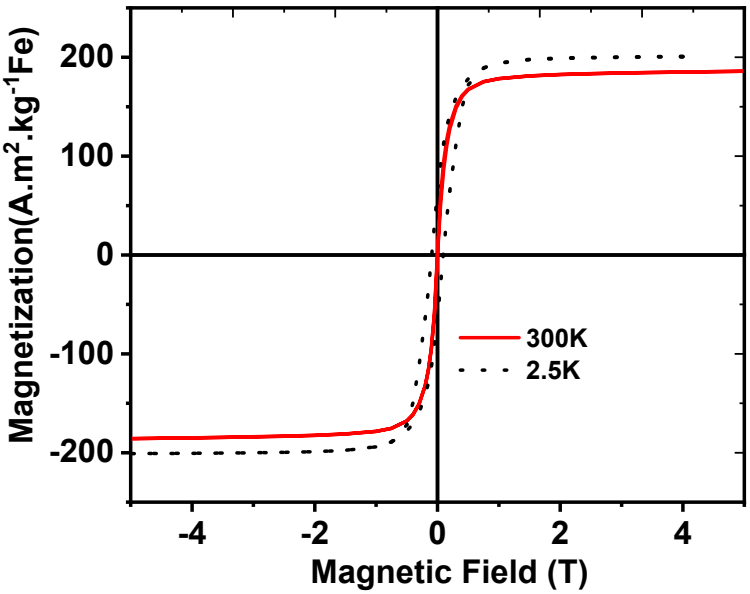

Fig. SI1 Magnetization curves of the ZVFeNPs recorded at 2.5 K (dotted line) and 300 K (solid line).

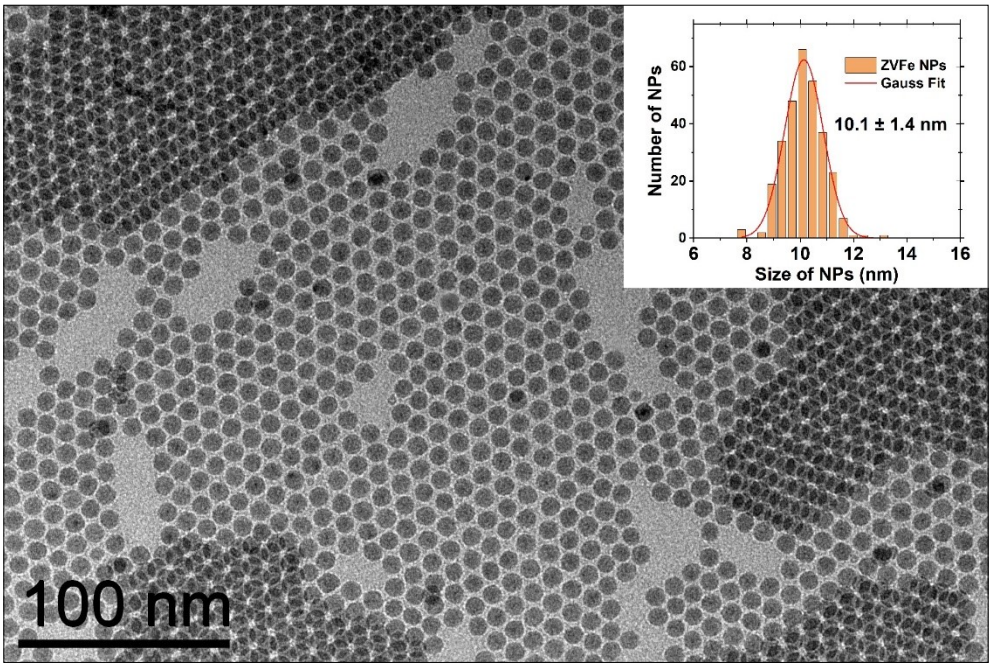

Fig. SI2 Typical TEM image of the ZVFeNPs and corresponding size histogram.

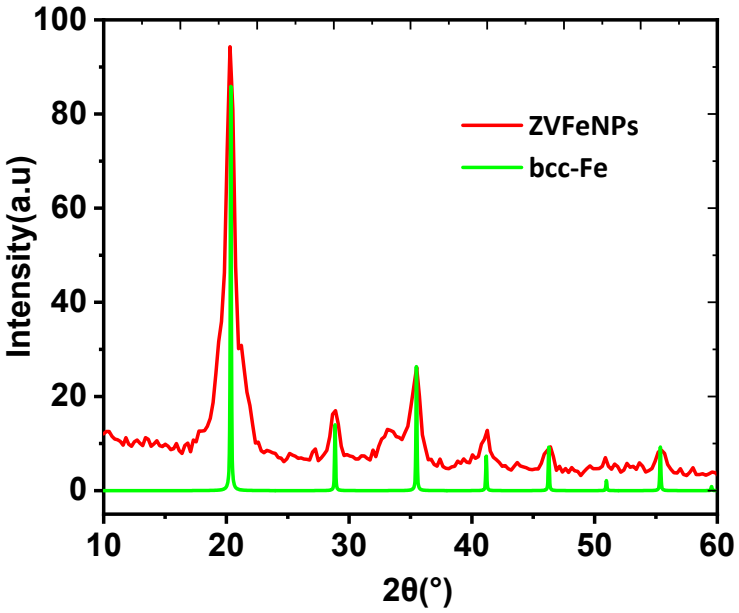

Fig. SI3 XRD diagram of the ZVFeNPs and reference data for bcc-Fe (ICSD 44863).

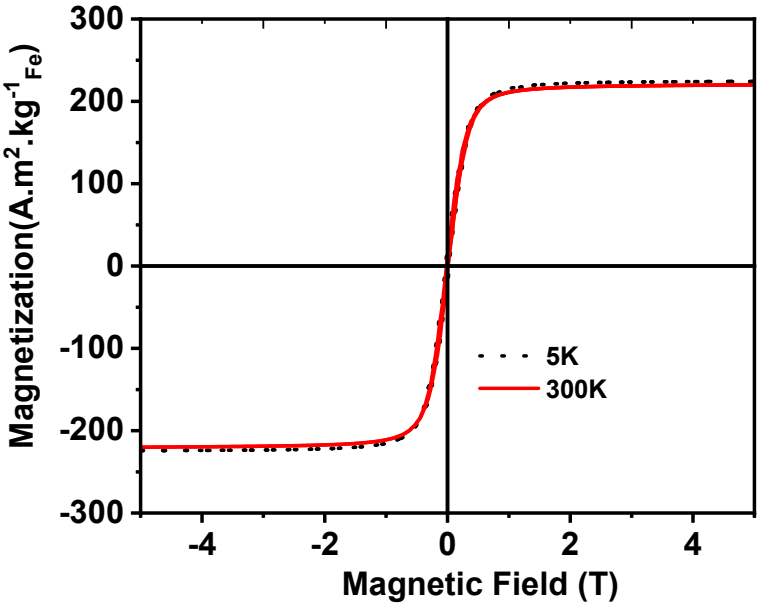

Fig. SI4 Magnetization curves of **sample H** recorded at 5 K (dotted line) and 300 K (solid line).

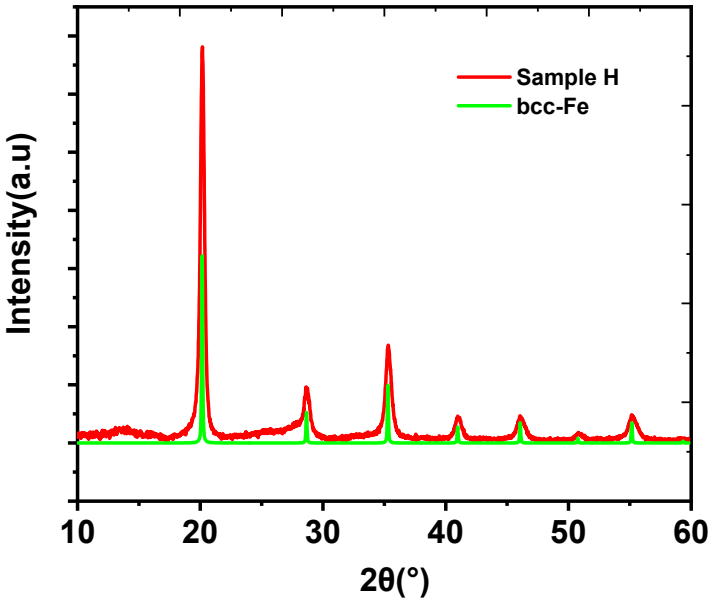

Fig. SI5 XRD diagram of **sample H** and reference data for bcc-Fe (ICSD 44863).

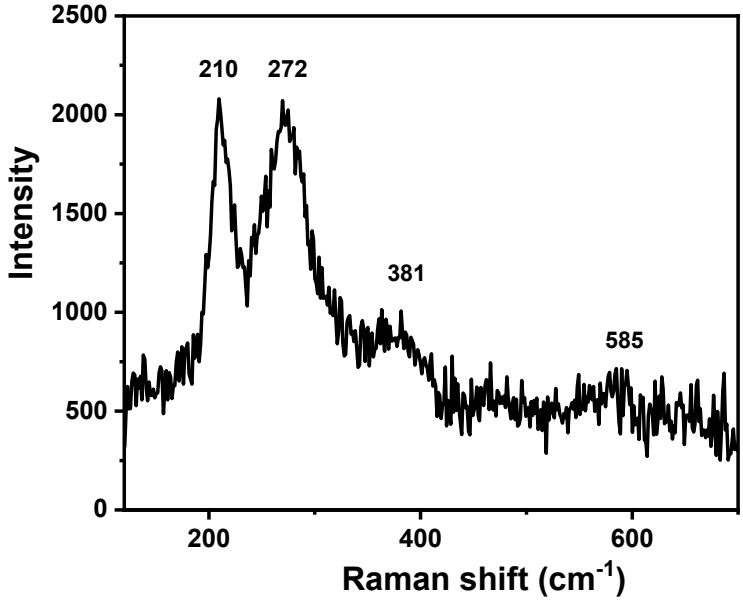

Fig. SI6 Raman spectrum of **sample N** (λ_{ex} = 532 nm, P = 2.6 mW).

Rietveld refinement conditions and results (including **Fig. SI7**)

- Diffractometer name and model : Panalytical MPDPro
- Radiation wavelength (Å): 0.709319
- Temperature of data collection : 293 K
- Step size: 0.016
- Chemical formula and formula weight (M): Fe6.00N2.94, M = 376.2617 g/mol
- Space group (No.) P 3 1 2 (149)
- Lattice parameters
  - a/ Å 4.798817
  - b/ Å 4.798817
  - c/ Å 4.419257
  - alpha/ ° 90
  - beta/ ° 90
  - gamma/ ° 120
  - V/ 10^6 pm^3 88.13497
- Number of formula units in unit cell (Z) : 1
- Number of reflections : 641
- Final R values (Rwp, Rexp and Rl) and method of background treatment:
  - Profile function: Pseudo Voigt
  - Background: Polynomial
  - R (expected)/ %: 3.33850
  - R (profile)/ %: 5.83257
  - R (weighted profile)/ %: 5.86908

- Occupancy, atomic fract. coordinates and Biso for 33575-ICSD

Atom	Wyck.	s.o.f.	x	y	z	B/ 10^4 pm^2
Fe1	6l	1.000000	0.000000	0.333300	0.250000	0.050000
N1	1a	1.000000	0.000000	0.000000	0.000000	0.050000
N2	1e	1.000000	0.666667	0.333333	0.000000	0.050000
N3	1d	0.940000	0.333333	0.666667	0.500000	0.050000

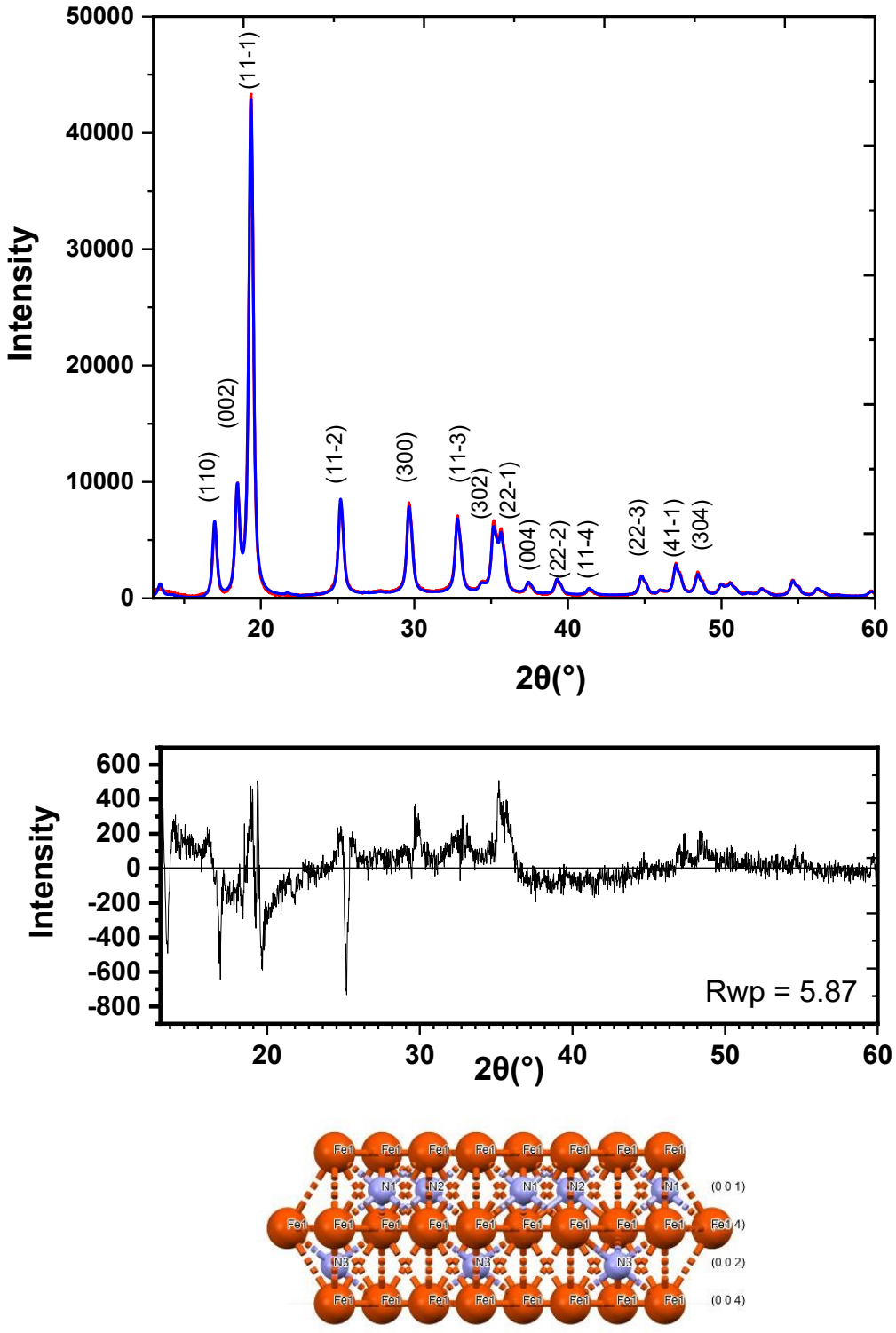

Fig. SI7 top: Rietveld refined XRD diagram of sample N (red: experimental; blue: calculated); middle: residue from the fit; bottom: schematic representation of the ε structure highlighting the (002) plane of N3 atoms.

Mössbauer spectroscopy (including **Table SI1** and **Fig. SI8**)

The best fit of the experimental data could be achieved by taking into account a set of contributions characteristics of ε-$Fe_{2+x}N$, where $x \leq 0.2$.[1,2] Best fit was obtained considering the contributions of two kind of paramagnetic species with an isomer shifts of 0.52 and 0.45 mm/s, with quadrupolar splitting 0.23 and 0.42 respectively (Table SI1). Note the presence of a broad contribution related to ferromagnetic like nanoparticles, with a broad hyperfine field distribution from 3 to 32T (See Table SI1 and Fig. SI8). Since the Curie temperature of these materials is less or close to the Mössbauer spectrum measurement temperature (80K), for ε-$Fe_{2+x}N$ material with $x \leq 0.2$,[3] such a paramagnetic like behavior or broadened distribution of hyperfine field for the ferromagnetic contribution are expected, as a consequence of superparamagnetic relaxation in nanoparticles.

Table SI1 Mössbauer spectra parameters

Component	Isomeric shift ($mm.s^{-1)}$	Quadrupolar coupling ($mm.s^{-1}$)	Hyperfine field (T)	Weighted contribution to the fit
ε-Fe_2N - PM	0.52	0.23	0	41 %
	0.45	0.42	0	18 %
ε-Fe_2N - FM	0.35	0	Fig. SI8	41 %

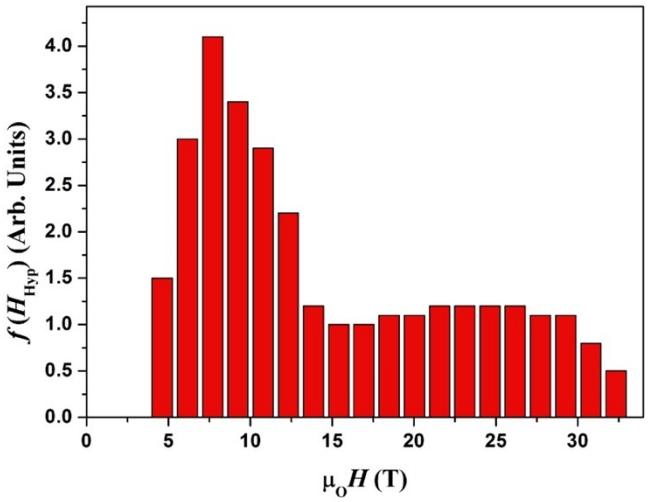

Fig. SI8 Distribution of hyperfine fields of the ε-Fe_2N ferromagnetic phase.

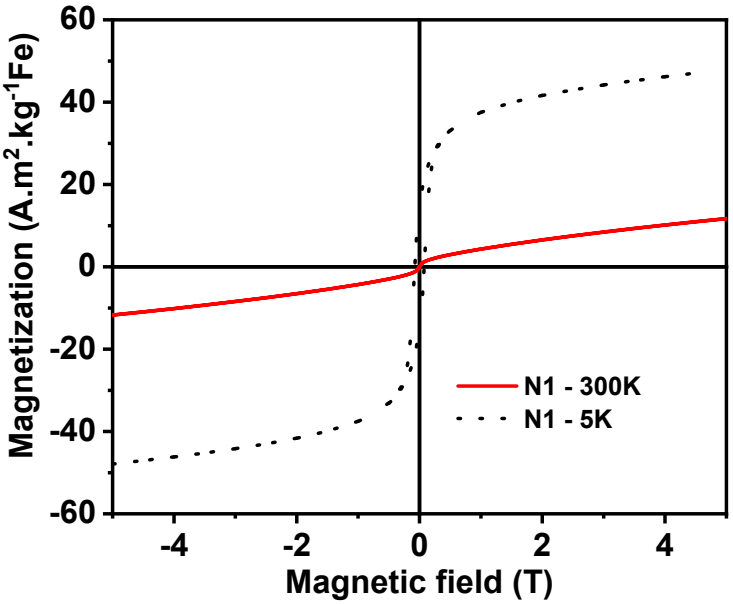

Fig. SI9 Typical hysteresis cycle recorded at 5K (dotted line) and 300K (solid line)

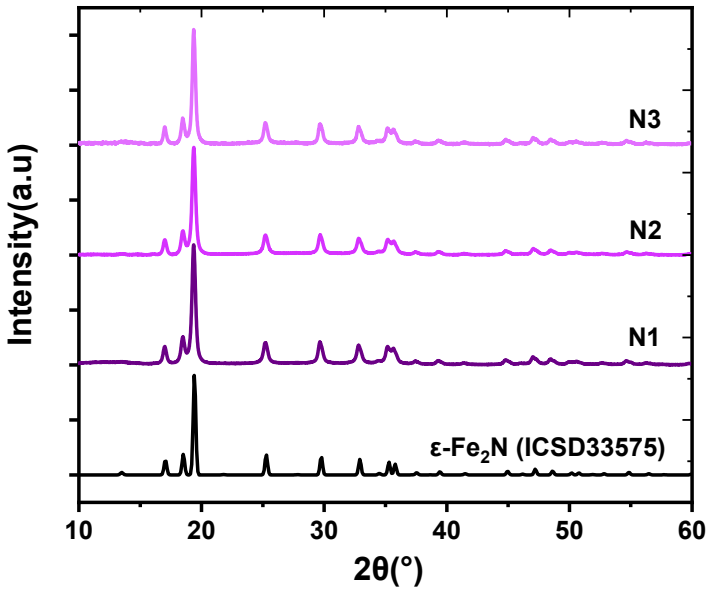

Fig. SI10 Comparison of the XRD diagrams of 3 different batches of Fe_2N nanomaterials.

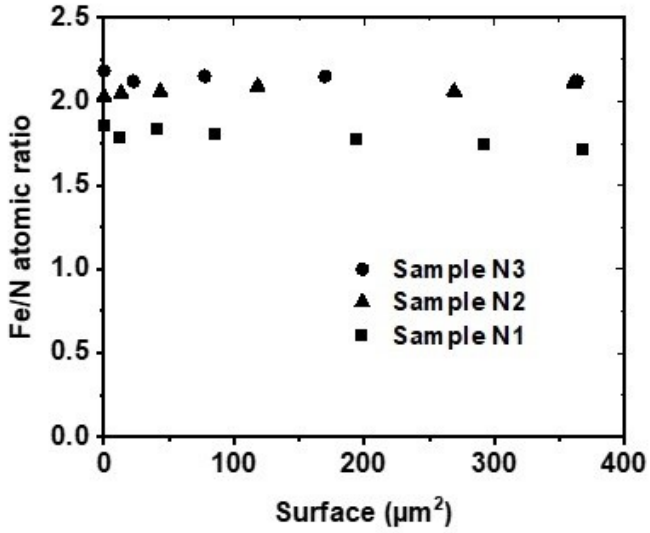

Fig. SI11 EDX analysis of 3 different batches of Fe_2N nanomaterials.

Table SI2 Main characteristics of typical batches of nitridated nanomaterials.

Sample	N1	N2	N3	N-FTO
Crystallite size (nm)	15±1	15±1	14±1	10±1
Crystallographic phase /space group	ε-Fe_2N / P312	ε-Fe_2N / P312	ε-Fe_2N / P312	ε-Fe_2N / P312
a(nm)	0.48011	0.47982	0.48032	0.47972
b(nm)	0.48011	0.47982	0.48032	0.47972
c(nm)	0.44252	0.44224	0.44194	0.44203
Fe/N atomic ratio (Vegard law)	2.04	2.06	2.05	2.07
Fe/N atomic ratio (EDX)	2.1	2	1.8	2.3
Magnetization (A.m².kg_{Fe}^{-1} at 5T and 5K)	47±2	45±2	47±2	not measured

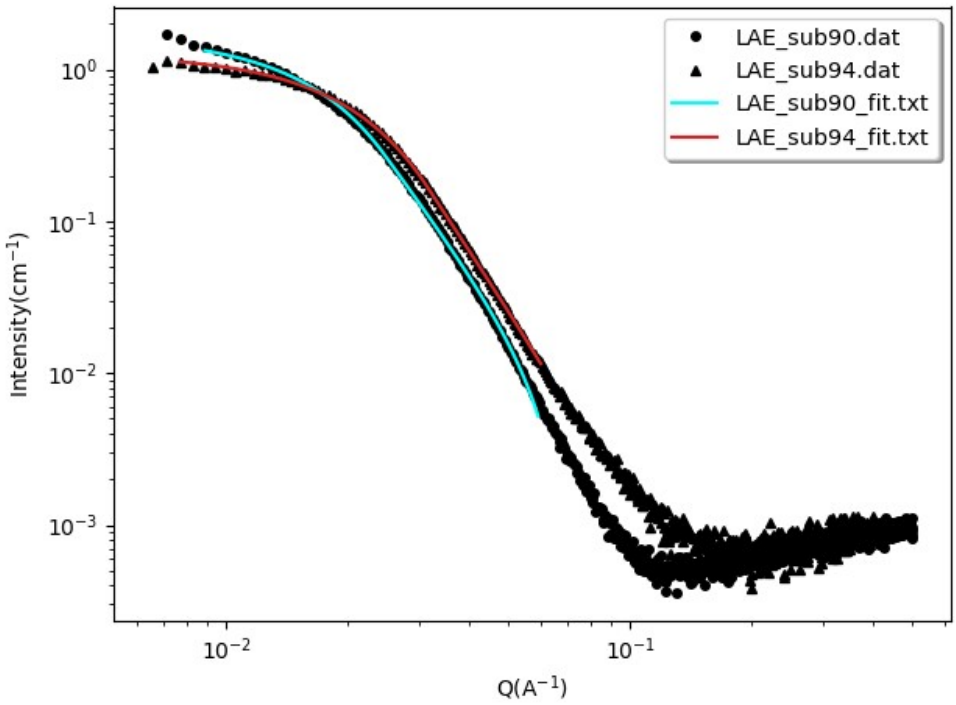

	LAE90_sub.dat	**LAE94_sub.dat**
Gyration radius (nm)	9.1	7.9
Porod value	4.0	4.0

Fig. SI12 SAXS measurements on two different batches of nitridated material (dots) and corresponding fits (solid lines)

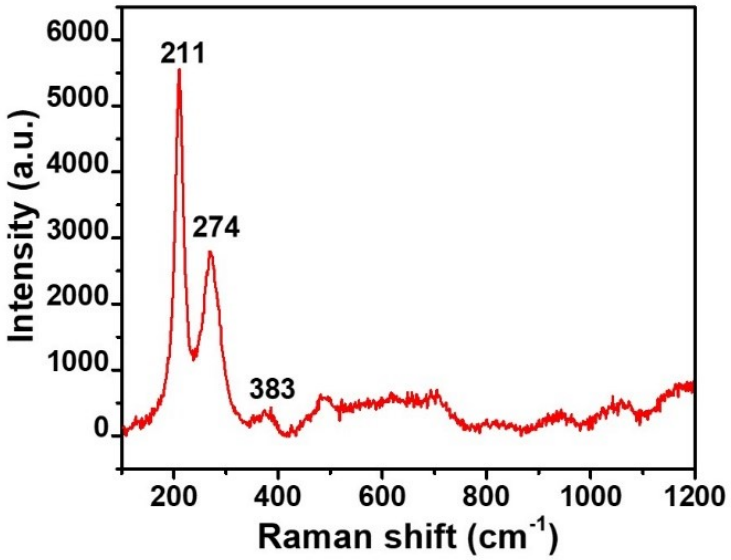

Fig. S13 Raman spectrum of sample Fe_2N/FTO (λ_{ex} = 523 nm, P = 10 mW).

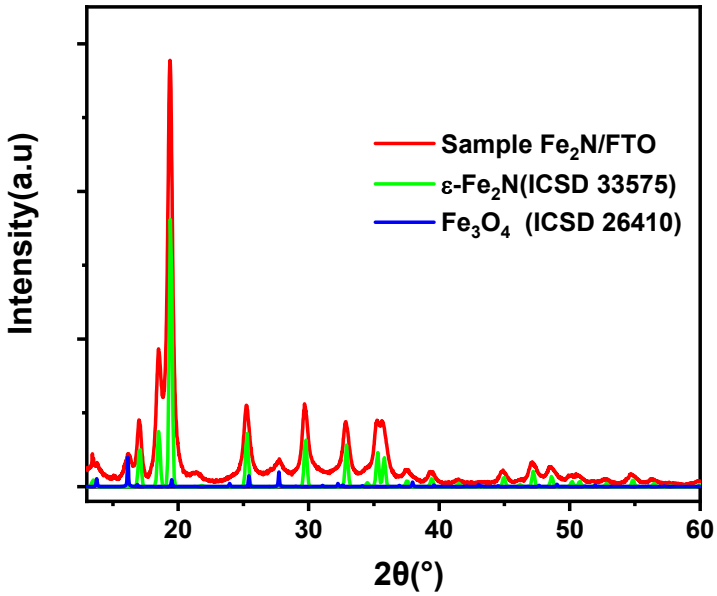

Fig. SI14 XRD diagram of sample Fe_2N/FTO and reference data for ε-Fe_2N (ICSD33575).

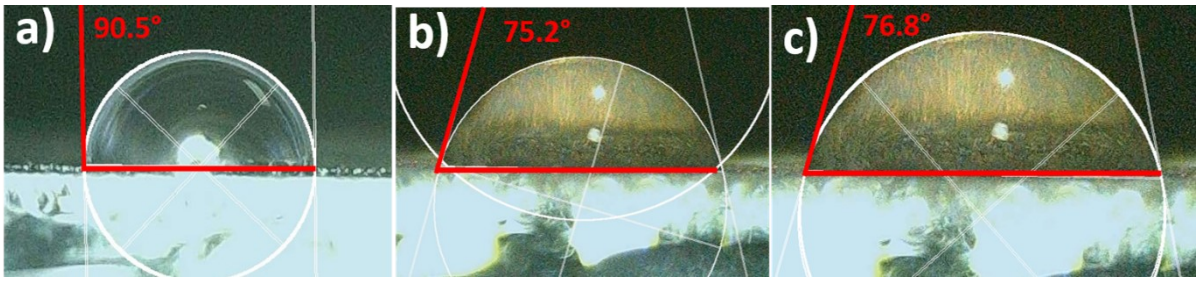

Fig. SI15 Water contact angle measured for: a) a freshly prepared Fe_2N/FTO catalyst electrode; b) the activated Fe_2N/FTO catalyst electrode; c) the activated Fe_2N/FTO catalyst electrode that experienced a partial detachment of catalyst upon increasing the number of potential polarizations.

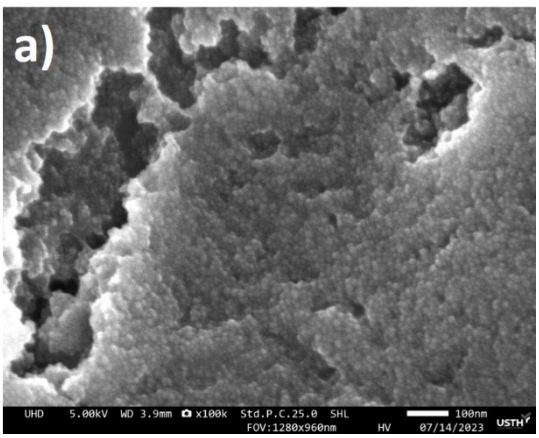

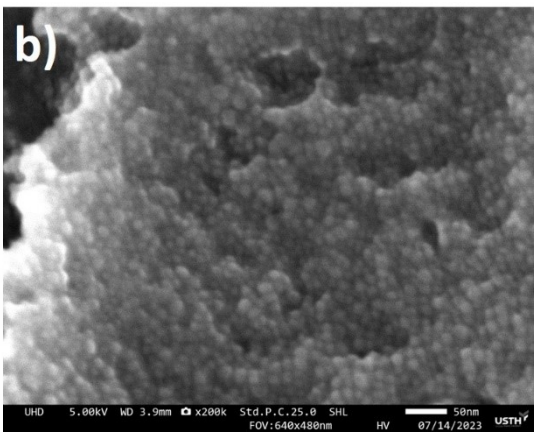

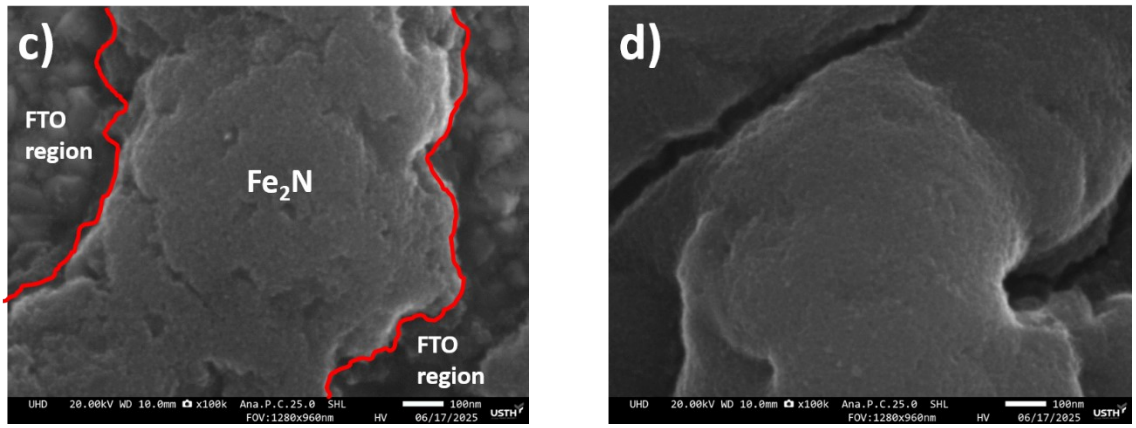

Fig. SI16 SEM images recorded on an as-prepared Fe_2N/FTO catalyst electrode (a, b) and an activated Fe_2N/FTO catalyst electrode (c, d) at different magnifications.

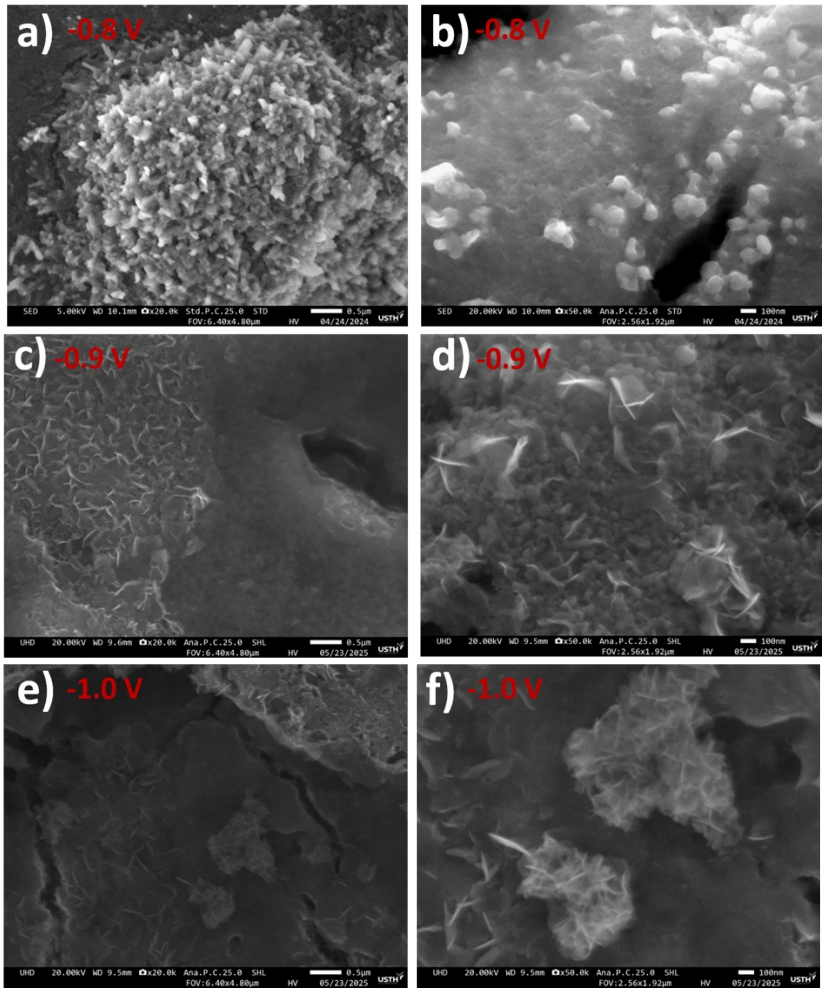

Fig. SI17 SEM images taken on a ε-Fe_2N/graphite electrode after being conditioned at -0.8 V (a, b); -0.9 V (c, d) and -1.0 V *vs.* RHE (e, f) for 1.5 hours. Electrolyte was a 0.1 M $NaHCO_3$ solution saturated with CO_2. a), c), and e) : scale bar 0.5 µm ; b), d), f) : scale bar 100 nm.

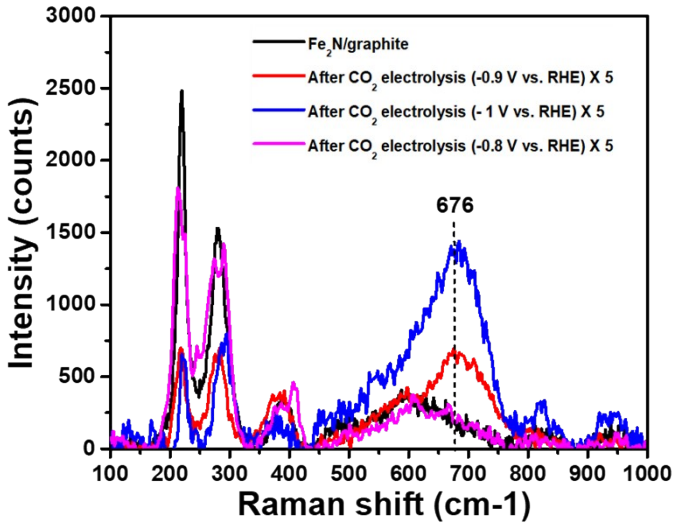

Fig. SI18 Raman spectra recorded for an as-prepared ε-Fe_2N/graphite electrode (black trace) and a ε-Fe_2N/graphite catalyst electrode after being conditioned -0.8 V (pink trace), -0.9 V (red trace) and -1.0 V vs. RHE (blue trace) in a 0. 1 M $NaHCO_3$ solution saturated with CO_2.

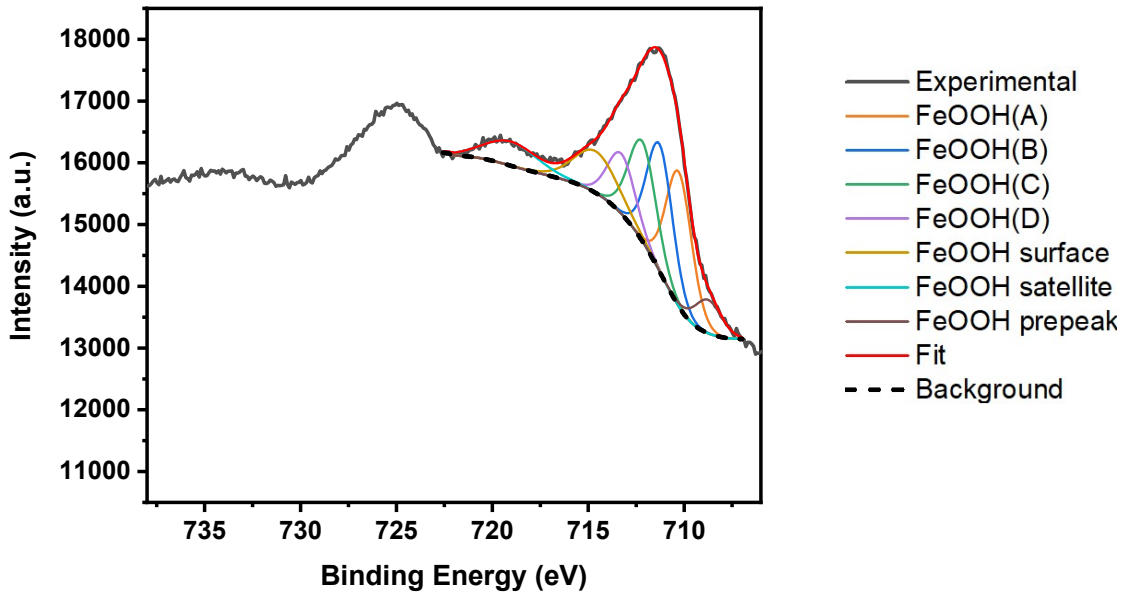

Fig. S19 Fe2p XPS spectrum of the ε-Fe_2N/graphite catalyst electrode after being conditioned -0.8 V in a 0.1 M $NaHCO_3$ solution saturated with CO_2, as well as best fit achieved in the $Fe2p_{3/2}$ region (background in black dashed line).